MCG 5125-Advanced Dynamics Project Part 1&2: Modeling of a Floating Wind Turbine In Aspect of Rigid and Deformable Dynamics

Runnan Zou
Department of Mechanical Engineering
University of Ottawa

***Abstract*—In order to gain an insight into the dynamics of the floating wind turbine in the aspect of rigid and deformable body dynamics, this report put forward a simplified dynamic model of floating wind turbine and an analysis of its deformable tower. Firstly, a simulation is carried out on the hypothesis that each part of the floating wind turbine is rigid. The analysis of the system is built based on Lagrange equation. Secondly, a Timoshenko beam model of the deformable tower is carried out based on Hamilton's principle and Galerkin projection. After simulation in MATLAB/Simulink, the results are analyzed and discussed. The simulation results are verified to have a certain accuracy.**

Keywords—rigid body dynamics, deformable-body analysis, floating wind turbine, simplified model, Simulink, MATLAB

I. Description of the Floating Wind Turbine System

In this report, a wind turbine that is floating in the sea is introduced and modeled. With the growing concern of energy and the environment, wind energy has drawn great attention since it is renewable and clean. As non-polluting and inexhaustible energy that could be renewed and acquired everywhere on earth, wind power has been deemed as alternative energy for conventional energy generation.

The wind turbines are always built in windy onshore land or offshore windy field. In open grassland and plains, thousands of wind turbines have been built to obtain the abundant wind energy there. The offshore wind field is widely spread all over the world with a relatively low exploiting rate [1]. With the advantage of high mean wind speed, low turbulence, and low wind shear, an offshore wind field is an ideal place for wind power generation. However, the environment of the offshore wind field is complicated with the wind, wave and other environmental factors which bring challenge and requirements for the design of floating wind turbine. One of the requirements for the deep-water offshore floating wind turbine is the reliable structure that is capable of supporting the equipment above. A cost-effective floating wind turbine with high integrity of structural dynamics is necessary to be established.

Traditionally, the floating wind turbine is designed in spar-buoy type, semi-submersible type, tension leg platform type, and barge type. The spar-buoy type has a thin and tall buyo with a long cylinder tank. The hydrodynamics stability is maintained by lowering the center of mass to beneath the buoyance tank [2]. The semi-submersible platform is widely applied in the field of offshore drilling and oil production platform. The buoyance of a semi-submersible platform is generated by the wave and watertight pontoons located below the ocean surface which enables the deck locates above the surface of the ocean [3-5]. The tension leg platform, which is a vertically moored floating structure, is moored by tension legs for the purpose of eliminating all vertical motion of the platform [6-8]. In this report, the floating wind turbine is designed in a type of spar-buyo.

The floating wind turbine consists of blades, nacelle, tower, platform, and moorings. The blade receives the energy generated by wind and transfers it towards the electricity generator by a gearbox. The tower and platform are responsible for the stability of the whole system. The efficiency of the system is affected by the power generating module and the stability of the system.

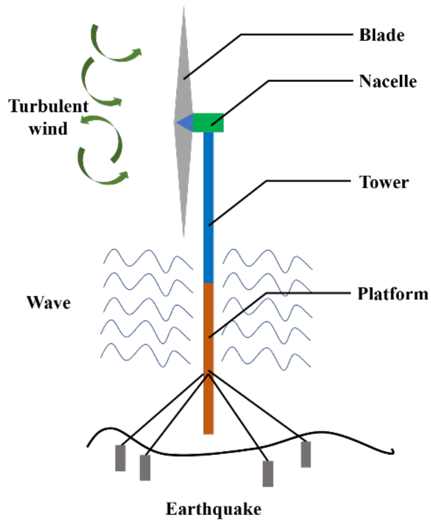

Fig. 1. Structure of the floating wind turbine

In part 1 of the project, the simplified dynamics model is built in MATLAB/Simulink. In the article we investigate, a tuned mass damper (TMD) is employed in the system to reduce the vibration of the wind turbine. The application of a tuned mass damper could significantly reduce the amplitude of the vibration of the system [9-10]. Therefore, the parameters of the tuned mass damper are worth to be investigated. The base of this research is the modeling of the floating wind turbine system with accuracy.

In part 2 of the project, the tower of the wind is identified as a slender deformable part. In the article [11-12], the deformable characteristic of the tower of the wind turbine that built in soil was investigated based on the model of Timoshenko beam. Researchers built a thorough model of the wind turbine in ocean with the considering of Hyperelastic law [13]. In the paper [14], the mathematical model of the Timoshenko beam was deeply discussed. The model that is picked out for this tower is the Timoshenko beam since the deformation of the beam in the beam in direction of axis could not be ignored. The simplified deformable model of the beam is built in MATLAB/Simulink. In this modeling of the beam, the finite element method is applied based on Galerkin projection.

II. MODELING ASSUMPTIONS

In the offshore wind field, the main impact applied on the turbine is turbulent wind, tidal and storm surge, currents, and ship and ice impacts. The factors that need to be concerned are complicated while developing a vibration control scheme for the stabilization of the floating wind turbine. Therefore, a simplified model of floating wind turbine is carried out based on the hypothesis that all parts of the turbine are rigid. The effect applied on the tower, platform, and TMD are transferred to the effect generated by spring and damper.

The simplified model of floating wind turbine is shown in Figure 2.

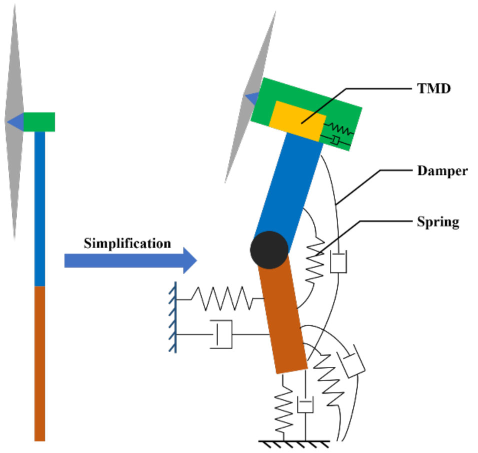

Fig. 2. Simplification of the floating wind turbine

There are 5 degrees of freedom of the simplified model:

$$q = (\theta_P, \theta_T, x_{TMD}, x_P, z_P)$$

where θ_P is the angular displacement of the platform from the axis y, θ_T is the angler displacement of the tower from the axis y, x_{TMD} is the linear displacement of the center of the tuned mass damper in x, x_P is the linear displacement of the center of the platform in x, z_P is the linear displacement of the center of the platform in z. The origin of the global coordinate system is located on the joint between tower and platform.

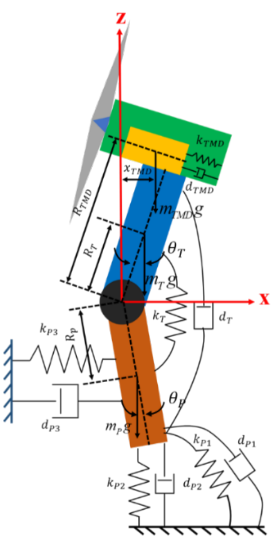

Fig. 3. Simplification of floating wind turbine with details

The detail of the model is shown in Figure 3. k_{TMD} is the stiffness of the spring attached to the tuned mass damper, d_{TMD} is the damping coefficient of the damper attached to the tuned mass damper, m_{TMD} is the mass of the tuned mass damper, R_{TMD} is the distance between the tuned mass damper and the origin of the coordinate. m_T is the mass of the tower, k_T is the stiffness of the spring attached to the tower and platform, d_T is the damping coefficient of the damper attached to the tower and platform, R_T is the distance between the mass center of tower and the origin of the coordinate. R_P is the distance between the mass center of platform and the origin of the coordinate, m_P is the mass of the platform. k_{P1}, k_{P2}, k_{P3} simulate the spring stiffness of the platform pitching, heaving and surging movements. d_{P1}, d_{P2}, d_{P3} simulate the damping coefficient of the platform pitching, heaving and surging movements. With the method of Lagrange equation:

$$\begin{cases} \dfrac{d}{dt}\left(\dfrac{\partial L}{\partial \dot{q}_i}\right) - \left(\dfrac{\partial L}{\partial q_i}\right) = Q_i \quad i = 1,2,3... \\ L = T - V \end{cases} \tag{1}$$

where T denotes the total kinematic energy of the system, V is the total potential energy of the system, L is the Lagrange operator. q_i and $\dot{q}_i$ are the generalized coordinate and derivatives of the generalized coordinate by time. Q_i is the generalized force.

In the Lagrange equation, the kinetic energy T of the system contains the kinematic energy of tower, platform and tuned mass damper which are:

$$\begin{aligned} &T_T = 0.5 I_T \dot{\theta}_T^2 \\ &T_P = 0.5 I_P \dot{\theta}^2 + 0.5 m_P(\dot{x}_P^2 + \dot{z}_P^2) \\ &T_{TMD} = 0.5 m_{TMD} \dot{x}_{TMD}^2 + 0.5 m_T(\dot{x}_P^2 + 2\dot{x}_P R_T \dot{\theta}_T cos\theta_T + R_T^2 \dot{\theta}_T^2 + \dot{z}_P^2 - 2\dot{z}_P R_T \dot{\theta}_T sin\theta_T) \end{aligned} \tag{2}$$

By combining the kinematic energy of tower, platform, and tuned mass damper, we could acquire the kinematic energy of the system is:

$$\begin{aligned} T = {} & 0.5 I_T \dot{\theta}_T^2 + 0.5 I_P \dot{\theta}_P^2 + 0.5 m_{TMD} \dot{x}_{TMD}^2 + 0.5 m_P(\dot{x}_P^2 + \dot{z}_P^2) \\ & + 0.5 m_T(\dot{x}_P^2 + 2\dot{x}_P R_T \dot{\theta}_T cos\theta_T + R_T^2 \dot{\theta}_T^2 + \dot{z}_P^2 - 2\dot{z}_P R_T \dot{\theta}_T sin\theta_T) \end{aligned} \tag{3}$$

where I_T is the inertia moment of tower, I_P is the inertia moment of platform.

The potential energy of the system contains two parts, gravitational potential energy and elastic potential energy which are shown as follows in each part of the system.

$$\begin{aligned} &V_{GT} = m_T g R_T cos\theta_T \\ &V_{ET} = 0.5 k_T(\theta_T - \theta_P)^2 \\ &V_{GP} = -m_P g R_P cos\theta_P \\ &V_{EP} = 0.5 k_{P1}\theta_P^2 + 0.5 k_{P3} x_P^2 + 0.5 k_{P2} z_P^2 \\ &V_{GTMD} = m_{TMD} g [R_{TMD} cos\theta_T + (x_{TMD} - R_{TMD} sin\theta_T) tan\theta_T] \\ &V_{ETMD} = 0.5 k_{TMD}(x_{TMD} - R_{TMD} sin\theta_T - x_P)^2 \end{aligned} \tag{4}$$

where V_{GT} is the gravitational potential energy of the tower and V_{ET} elastic potential energy of the tower. V_{GP} is the gravitational potential energy of the platform and V_{EP} elastic potential energy of the platform. V_{GTMD} is the gravitational potential energy of the TMD and V_{ETMD} elastic potential energy of the TMD.

By adding the above potential energy together, the potential energy V of the system is:

$$
\begin{aligned}
V &= 0.5k_T(\theta_T-\theta_P)^2+0.5k_{TMD}(x_{TMD}-R_{TMD}sin\theta_T-x_P)^2 \\
&+0.5k_{P1}\theta_P^2+m_TgR_Tcos\theta_T-m_PgR_Pcos\theta_P+m_{TMD}g[R_{TMD}cos\theta_T \\
&+(x_{TMD}-R_{TMD}sin\theta_T)tan\theta_T]+0.5k_{P3}x_P^2+0.5k_{P2}z_P^2
\end{aligned}
\tag{5}
$$

For the non-conservative force, the damper force is the only one applied to the system. Based on the virtual work theorem, the calculation of the generalized non-conservative force is:

$$
\begin{cases}
Q_{\theta_T} = -d_T(\dot{\theta}_T-\dot{\theta}_P)+ \\
d_{TMD}R_{TMD}cos\theta_T(\dot{x}_{TMD}- \\
R_{TMD}\dot{\theta}_Tcos\theta_T-\dot{x}_P) \\
Q_{\theta_P} = d_T(\dot{\theta}_T-\dot{\theta}_P)-d_{P1}\dot{\theta}_P \\
Q_{x_{TMD}} = -d_{TMD}(\dot{x}_{TMD}- \\
R_{TMD}\dot{\theta}_Tcos\theta_T-\dot{x}_P) \\
Q_{x_P} = d_{TMD}(\dot{x}_{TMD}- \\
R_{TMD}\dot{\theta}_Tcos\theta_T-\dot{x}_P)-d_{P3}\dot{x}_P \\
Q_{z_P} = -d_{P2}\dot{z}_P
\end{cases}
\tag{6}
$$

Substituting equation (2), (3) and (4) into (1), equations of the dynamic system is:

$$
\begin{cases}
I_T\ddot{\theta}_T = -d_T(\dot{\theta}_T-\dot{\theta}_P)-m_T(\ddot{x}_PR_Tcos\theta_T+2R_T^2\dot{\theta}_T-2\ddot{z}_PR_Tsin\theta_T \\
-\dot{z}_PR_T\dot{\theta}_Tcos\theta_T)-k_T(\theta_T-\theta_P)+k_{TMD}R_{TMD}(x_{TMD}-R_{TMD}sin\theta_T-x_P)cos\theta_T \\
+m_TgR_Tsin\theta_T-m_{TMD}g(-3R_{TMD}sin\theta_T+x_{TMD}) \\
+d_{TMD}R_{TMD}(\dot{x}_{TMD}-R_{TMD}\dot{\theta}_T-\dot{x}_P)cos\theta_T \\
I_P\ddot{\theta}_P = k_T(\theta_T-\theta_P)-k_{P1}\theta_P-m_PgR_Psin\theta_P+d_T(\dot{\theta}_T-\dot{\theta}_P)-d_{P1}\dot{\theta}_P \\
m_{TMD}\ddot{x}_{TMD} = -k_{TMD}(x_{TMD}-R_{TMD}\theta_T-x_P)+m_{TMD}gsin\theta_T+m_{TMD}gtan\theta_T \\
-d_{TMD}(\dot{x}_{TMD}-R_{TMD}\dot{\theta}_Tcos\theta_T-\dot{x}_P) \\
(m_T+m_P)\ddot{x}_P = -m_TR_T\ddot{\theta}_Tcos\theta_T+m_TR_T\dot{\theta}_T^2sin\theta_T+k_{TMD}(x_{TMD}-R_{TMD}sin\theta_T-x_P)-k_{P3}x_P \\
+d_{TMD}(\dot{x}_{TMD}-R_{TMD}\dot{\theta}_Tcos\theta_T-\dot{x}_P)-d_{P3}\dot{x}_P \\
(m_T+m_P)\ddot{z}_P = m_TR_T\ddot{\theta}_Tsin\theta_T+m_TR_T\dot{\theta}^2cos\theta_T-k_{P2}z_P-d_{P2}\dot{z}_P
\end{cases}
\tag{7}
$$

Since the vibration of the tower is no more than 10°, the condition $cos\theta_t \approx 1$ and $sin\theta_t \approx 0$, the equations can be simplified to:

$$
\begin{cases}
I_T\ddot{\theta}_T = -d_T(\dot{\theta}_T-\dot{\theta}_P)-m_T(\ddot{x}_PR_T+2R_T^2\dot{\theta}_T-2\ddot{z}_PR_T\theta_T \\
-\dot{z}_PR_T\dot{\theta}_T)-k_T(\theta_T-\theta_P)+k_{TMD}R_{TMD}(x_{TMD}-R_{TMD}\theta_T-x_P) \\
+m_TgR_T\theta_T-m_{TMD}g(-3R_{TMD}\theta_T+x_{TMD})+d_{TMD}R_{TMD}(\dot{x}_{TMD}-R_{TMD}\dot{\theta}_T-\dot{x}_P) \\
I_P\ddot{\theta}_P = k_T(\theta_T-\theta_P)-k_{P1}\theta_P-m_PgR_P\theta_P+d_T(\dot{\theta}_T-\dot{\theta}_P)-d_{P1}\dot{\theta}_P \\
m_{TMD}\ddot{x}_{TMD} = -k_{TMD}(x_{TMD}-R_{TMD}\theta_T-x_P)+m_{TMD}g\theta_T-d_{TMD}(\dot{x}_{TMD}-R_{TMD}\dot{\theta}_T-\dot{x}_P) \\
(m_T+m_P)\ddot{x}_P = -m_TR_T\ddot{\theta}_T+m_TR_T\dot{\theta}_T^2\theta_T+k_{TMD}(x_{TMD}-R_{TMD}\theta_T-x_P)-k_{P3}x_P \\
+d_{TMD}(\dot{x}_{TMD}-R_{TMD}\dot{\theta}_T-\dot{x}_P)-d_{P3}\dot{x}_P \\
(m_T+m_P)\ddot{z}_P = m_TR_T\ddot{\theta}_T\theta_T+m_TR_T\dot{\theta}^2-k_{P2}z_P-d_{P2}\dot{z}_P
\end{cases}
\tag{8}
$$

The parameter for the simulation is shown in Table 1.

TABLE I. PARAMETERS IN SIMULATION

Parameters	Symbol	Value	Unit
Mass of platform	m_P	7466330	kg
Mass of tower	m_T	249718	kg
Mass of TMD	m_{TMD}	3000	kg
Distance from mass center of TMD to origin	R_{TMD}	90	m
Distance from mass center of tower to origin	R_T	45	m
Distance from mass center of platform to origin	R_P	40	m
Stiffness of spring on TMD	k_{TMD}	249890	N/m
Stiffness of spring on tower	k_T	989650	N/m
Stiffness of spring1 on platform	k_{P1}	1546330	N/m
Stiffness of spring2 on platform	k_{P2}	59800000	N/m
Stiffness of spring3 on platform	k_{P3}	500000	N/m
Damping coefficient of damper on TMD	d_{TMD}	531360	N/m
Damping coefficient of damper on tower	d_T	566900	N·s/m
Damping coefficient of damper1 on platform	d_{P1}	544600	N·s/m
Damping coefficient of damper2 on platform	d_{P2}	569900	N·s/m
Damping coefficient of damper3 on platform	d_{P3}	532400	N·s/m

III. ANALYSIS OF THE DEFORMABLE TOWER

In the offshore environment where the wind turbine is built, the wind intensity is strong which brings high advantage for the wind turbine while on the other hand, the tower of wind turbine suffers several force and moments which challenge the strength and durability of the tower.

The model of the beam is selected from the model of Euler beam or the model of Timoshenko beam. Considering the ratio of thickness and height of the tower as well as the deformation of the tower in shear movement, the model of wind turbine tower we choose here is the Timoshenko beam model.

Therefore, the modeling of tower in the aspect of deformation is necessary. Since the objective is the tower, the tower model is derived from the model of wind turbine with several simplifications as shown in Fig 4:

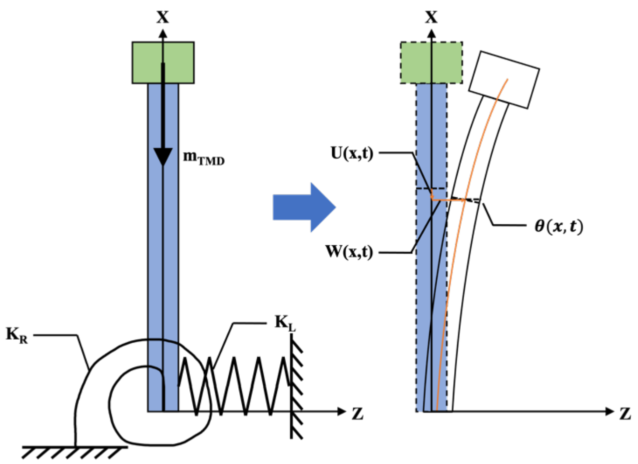

Fig. 4. Model of the deformable tower of the wind turbine

As it is shown in Fig 4, the connection between the platform and tower is simplified as the effect of a rotational string and a lateral string [15]. The force applied in the direction of axis x is the gravity of the TMD while the force applied in the direction of z axis is the wind force, since the wind is the offshore environment is strong in a wide range while the size of wind turbine is relatively small, the wind force applied on the tower is considered as an average force.

The potential energy of the tower is:

$$V=\frac{1}{2}\int_0^L\left(EA\left(u'\right)^2+EI\left(\theta'\right)^2+kGA\left(w'-\theta\right)^2\right)dx \tag{9}$$

where the L is the length of the tower, E is Young's modulus of the tower, A is cross-sectional area, k is shear coefficient, G is shear modulus of the tower material.

The kinematic energy of the tower is:

$$T=\frac{1}{2}\int_0^L\rho\left(A\left(\dot{u}^2+\dot{w}^2\right)+I_y\dot{\theta}^2\right)dx \tag{10}$$

where ρ is the density of the tower, I_y the moment inertia in the direction of y.

The work done by the non-conservative forces on the tower is:

$$\overline{\delta W}^{NC}=\int_0^L(f_w\delta w)dx+K_Lw(0,t)\delta w(0)+K_R\theta(0)\delta\theta(0)+m_{TMD}g\delta u(L,t) \tag{11}$$

where f_w is the average wind force applied on the tower, K_L is the lateral foundation stiffness, K_R is rotational foundation stiffness, m_{TMD} is the mass of the tower top, g is the gravity coefficient.

By applying the boundary equation derived from the simplification of the tower and the Hamilton principle, the weak form equation of the tower is shown as follows:

$$\begin{aligned}&\int_0^L\left(\rho A\ddot{w}\delta w+kGA\left(w'-\theta\right)\delta w'\right)dx+\int_0^L\left(\rho A\ddot{u}\delta u+EAu'\delta u'\right)dx+\int_0^L\left(\rho I\ddot{\theta}\delta\theta-kGA\left(w'-\theta\right)\delta\theta+EI\theta'\delta\theta'\right)dx\\&=\int_0^L(f_w\delta w)dx+K_Lw(0,t)\delta w(0)+K_R\theta(0)\delta\theta(0)+m_{TMD}g\delta u(L,t)\end{aligned} \tag{12}$$

After acquiring the weak form equation of the beam, the semi-discrete form of the tower is obtained through the method of Galerkin projection. Since the beam is deemed as a universal Timoshenko beam with the same material, the spatial basis function of u, w and θ are built as follows:

$$\begin{aligned}u_N(x,t)&=\sum_1^N\psi_{uj}(x)q_{uj}(t)\\w_N(x,t)&=\sum_1^N\psi_{wj}(x)q_{wj}(t)\\\theta_N(x,t)&=\sum_1^N\psi_{\theta j}(x)q_{\theta j}(t)\\\delta u_N(x,t)&=\sum_1^N\varphi_{uj}(x)\delta q_{uj}(t)\\\delta w_N(x,t)&=\sum_1^N\varphi_{wj}(x)\delta q_{wj}(t)\\\delta\theta_N(x,t)&=\sum_1^N\varphi_{\theta j}(x)\delta q_{\theta j}(t)\end{aligned} \tag{13}$$

Since both ends of the tower are not fixed to a steady point in the space, the projections exist in both end of the tower in u, w and θ.

By substituting the Galerkin projection of coordinates into the weak form to explore the arbitrariness the coefficient δq_{uj}, δq_{wj} and $\delta q_{\theta j}$, j=1,2,3…, the block matrix system is obtained as follows:

$$\begin{bmatrix}M_u&0&0\\0&M_w&0\\0&0&M_\theta\end{bmatrix}\begin{bmatrix}\ddot{q}_u\\\ddot{q}_w\\\ddot{q}_\theta\end{bmatrix}+\begin{bmatrix}K_u&0&0\\0&K_{w\theta}&0\\0&-K_{\theta w}&K_{\theta\theta}\end{bmatrix}\begin{bmatrix}q_u\\q_w\\q_\theta\end{bmatrix}=\begin{bmatrix}0\\F_w\\0\end{bmatrix}+\begin{bmatrix}F_{bu}\\F_{bw}\\F_{b\theta}\end{bmatrix} \tag{14}$$

where the block entries are given by,

$$\begin{aligned}M_u&=\int_0^L\rho A\psi_u\varphi_u dx\\M_w&=\int_0^L\rho A\psi_w\varphi_w dx\\M_\theta&=\int_0^L\rho A\psi_\theta\varphi_\theta dx\\K_u&=\int_0^L EA\psi_u'\varphi_u'dx\\K_{\theta w}&=\int_0^L kGA\psi_w'(\psi_w'-\psi_\theta)dx\\K_{w\theta}&=\int_0^L kGA\varphi_\theta(\psi_w'-\psi_\theta)dx\\K_\theta&=\int_0^L EI\psi_\theta'\varphi_\theta'dx\\F_w&=\int_0^L f_w\varphi_w dx\\F_{bu}&=m_{TMD}g\varphi_u(L)\\F_{bw}&=K_L\psi_w(0)\varphi_w(0)\\F_{b\theta}&=K_R\psi_\theta(0)\varphi_\theta(0)\end{aligned} \tag{15}$$

IV. NUMERICAL METHODS

The numerical method applied in this report is ODE45. ODE45 is a MATLAB solver for ordinary differential equations based on Runge-Kutta method. Runge-Kutta method is a kind of method for solving ordinary differential equations. With a problem as follows:

$$\frac{dy}{dt}=f(y,t),y(t_0)=y_0 \tag{16}$$

In order to find the y of time t, the solution step is defined as follows:

$$\begin{aligned}y_{n+1}&=y_n+\frac{1}{6}h(k_1+2k_2+3k_3+4k_4)\\t_{n+1}&=t_n+h\end{aligned} \tag{17}$$

where k_1, k_2, k_3, k_4 are as follows:

$$\begin{aligned}k_1&=f(t_n,y_n)\\k_2&=f(t_n+\frac{h}{2},y_n+\frac{k_1h}{2})\\k_3&=f(t_n+\frac{h}{2},y_n+\frac{k_2h}{2})\\k_4&=f(t_n+h,y_n+k_3h)\end{aligned} \tag{18}$$

Based on the core of Runge-Kutta method, ODE45 in MATLAB/Simulink is utilized for finding solution in this project.

V. SIMULATION RESULTS AND ANALYSIS

The model and simulation are built in MATLAB/Simulink with different sets of initial conditions in aspect of investigating the rigid body characteristic of the wind turbine structure and the deformable characteristic of the tower.

For the rigid body simulation, the above equation are built in models in Simulink is as follows:

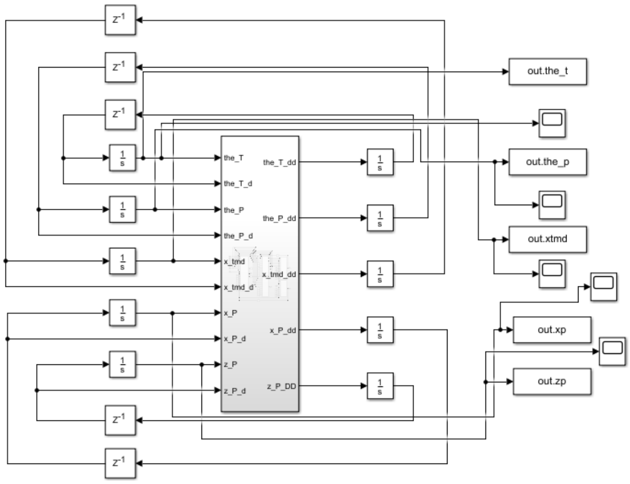

Fig. 5. Overall model for floating wind turbine in Simulink

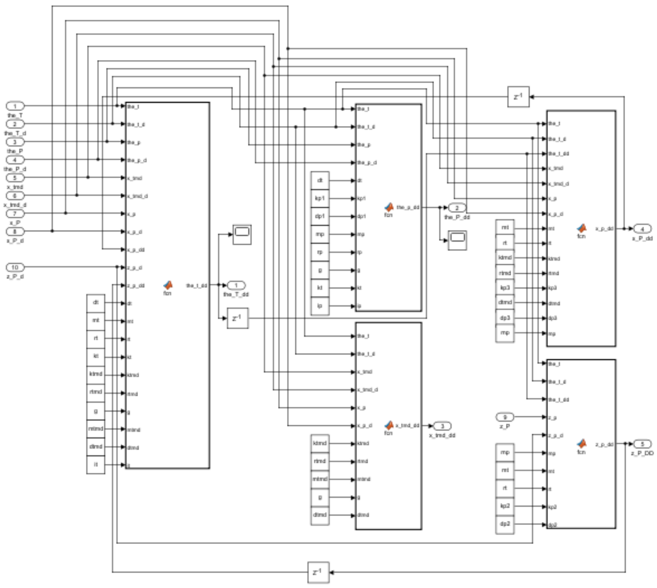

Fig. 6. Detailed model for floating wind turbine in Simulink

For the deformable tower model, the system is built as follows in the Simulink:

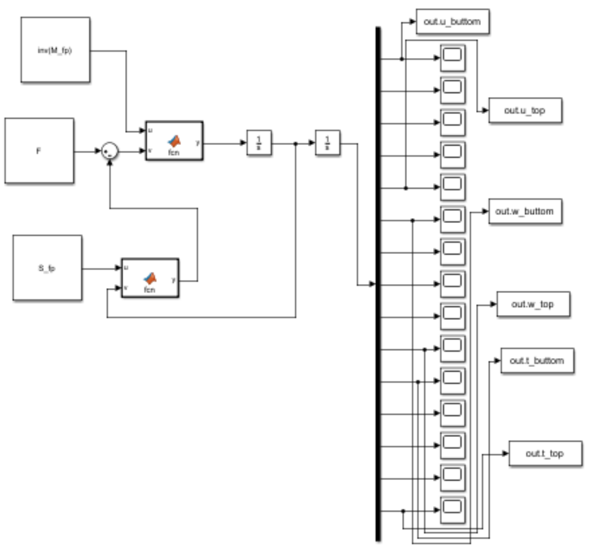

Fig. 7. Detailed model for the deformable tower of wind turbine generator

The simulation of the rigid body dynamics is set up in different scenarios. With the initial condition of (θ_P= 0,θ_T= 0, x_{TMD}= 0, x_P= 0, z_P= -20), the system dynamics are shown in Figure 6. As it is shown in the Figure 6, z_P and x_P goes to a stable value after several cycles of vibration. However, there are still some vibrations for θ_P, $\theta_T$and x_{TMD} which indicates that the parameters of the tuned mass damper need to be optimized afterward.

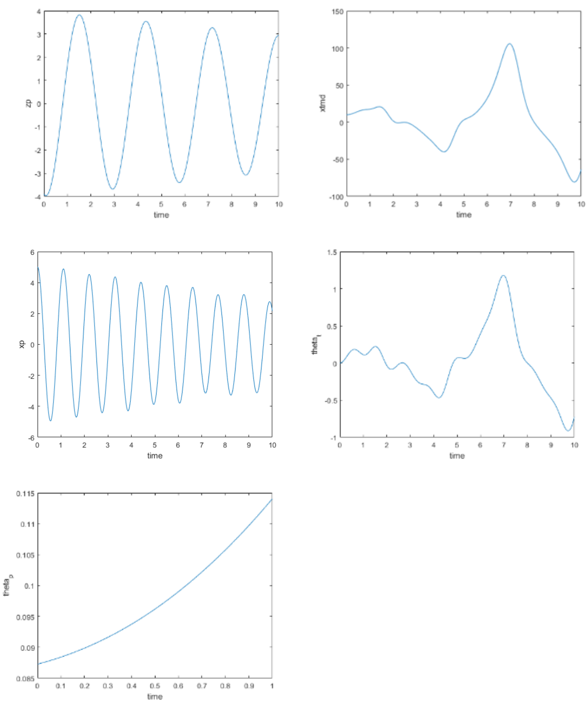

Fig. 8. Result of the first set of initial condition in Simulink

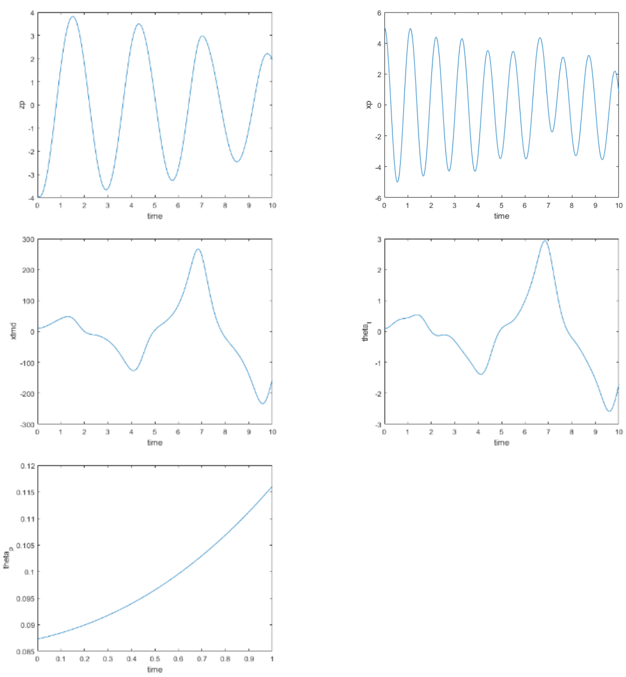

Fig. 9. Result of second set initial condition in Simulink

With the initial condition of (θ_P= 0,θ_T= 5°, x_{TMD}= 0, x_P= 0, z_P= -15), the system dynamics are shown in Figure 7. As it is shown in Figure 7, the result is quite similar to the first simulation. Therefore, the parameter of TMD is worth to be investigated in the base of the simulation. The initial condition, stiffness and damping coefficient are all have great influence on the response of the system.

The simulation of a deformable tower is carried out based on the initial condition of u = 0, w = 0, θ = 0. With the limit of computational capacity, the node number of the simulation is set as 5. The condition of the simulation is depicted as follows:

TABLE II. PARAMETERS IN SIMULATION

Parameters	Symbol	Value	Unit
Moment inertia	I	0.7	kg
Density of the tower	ρ	7800	kg/m^3
Mass of TMD	m_{TMD}	3000	kg
Cross-sectional area	A	12.56	m^2
Young's modulus	E	210	GPa
Shear coefficient	k	0.53	-
Length of the tower	L	90	m
Lateral foundation stiffness	K_L	4	GN/m
Rotational foundation stiffness	K_R	270	GNm/rad
Shear modulus of the tower material	G	79.3	GPa

Based on the above depiction of the scenario, the matrix of the modeling is shown as follows:

$$M=\begin{bmatrix}
32353.62 & 8466.37 & 0 & 0 & 0 & 0 & 0 & 0 & 0 & 0 & 0 & 0 & 0 & 0 & 0\\
8466.37 & 36284.44 & 9675.85 & 0 & 0 & 0 & 0 & 0 & 0 & 0 & 0 & 0 & 0 & 0 & 0\\
0 & 9675.85 & 35074.96 & 9675.85 & 0 & 0 & 0 & 0 & 0 & 0 & 0 & 0 & 0 & 0 & 0\\
0 & 0 & 9675.85 & 36284.44 & 8466.37 & 0 & 0 & 0 & 0 & 0 & 0 & 0 & 0 & 0 & 0\\
0 & 0 & 0 & 8466.37 & 32353.62 & 0 & 0 & 0 & 0 & 0 & 0 & 0 & 0 & 0 & 0\\
0 & 0 & 0 & 0 & 0 & 32353.62 & 8466.37 & 0 & 0 & 0 & 0 & 0 & 0 & 0 & 0\\
0 & 0 & 0 & 0 & 0 & 8466.370 & 36284.44 & 9675.85 & 0 & 0 & 0 & 0 & 0 & 0 & 0\\
0 & 0 & 0 & 0 & 0 & 0 & 9675.85 & 35074.96 & 9675.85 & 0 & 0 & 0 & 0 & 0 & 0\\
0 & 0 & 0 & 0 & 0 & 0 & 0 & 9675.85 & 36284.44 & 8466.37 & 0 & 0 & 0 & 0 & 0\\
0 & 0 & 0 & 0 & 0 & 0 & 0 & 0 & 8466.37 & 32353.62 & 0 & 0 & 0 & 0 & 0\\
0 & 0 & 0 & 0 & 0 & 0 & 0 & 0 & 0 & 0 & 1803.14 & 471.85 & 0 & 0 & 0\\
0 & 0 & 0 & 0 & 0 & 0 & 0 & 0 & 0 & 0 & 471.85 & 2022.22 & 539.25 & 0 & 0\\
0 & 0 & 0 & 0 & 0 & 0 & 0 & 0 & 0 & 0 & 0 & 539.25 & 1954.81 & 539.25 & 0\\
0 & 0 & 0 & 0 & 0 & 0 & 0 & 0 & 0 & 0 & 0 & 0 & 539.25 & 2022.22 & 471.85\\
0 & 0 & 0 & 0 & 0 & 0 & 0 & 0 & 0 & 0 & 0 & 0 & 0 & 471.85 & 1803.14
\end{bmatrix}$$

$$S=\begin{bmatrix}
3.1\times10^{13} & -3.1\times10^{13} & 0 & 0 & 0 & 0 & 0 & 0 & 0 & 0 & 0 & 0 & 0 & 0 & 0\\
-3.1\times10^{13} & 5.2\times10^{12} & -2.1\times10^{14} & 0 & 0 & 0 & 0 & 0 & 0 & 0 & 0 & 0 & 0 & 0 & 0\\
0 & -2.1\times10^{14} & 4.2\times10^{13} & -2.1\times10^{14} & 0 & 0 & 0 & 0 & 0 & 0 & 0 & 0 & 0 & 0 & 0\\
0 & 0 & -2.1\times10^{14} & 5.2\times10^{13} & -3.1\times10^{13} & 0 & 0 & 0 & 0 & 0 & 0 & 0 & 0 & 0 & 0\\
0 & 0 & 0 & -3.1\times10^{13} & 3.1\times10^{13} & 0 & 0 & 0 & 0 & 0 & 0 & 0 & 0 & 0 & 0\\
0 & 0 & 0 & 0 & 0 & 7.2\times10^{12} & -5.6\times10^{12} & 0 & 0 & 0 & 0 & 0 & 0 & 0 & 0\\
0 & 0 & 0 & 0 & 0 & -7.2\times10^{12} & 1.0\times10^{13} & -3.6\times10^{12} & 0 & 0 & 0 & 0 & 0 & 0 & 0\\
0 & 0 & 0 & 0 & 0 & 0 & -4.6\times10^{11} & 8.4\times10^{12} & -3.7\times10^{12} & 0 & 0 & 0 & 0 & 0 & 0\\
0 & 0 & 0 & 0 & 0 & 0 & 0 & -4.8\times10^{12} & 1.0\times10^{13} & -5.4\times10^{12} & 0 & 0 & 0 & 0 & 0\\
0 & 0 & 0 & 0 & 0 & 0 & 0 & 0 & -7.0\times10^{12} & 5.4\times10^{12} & 0 & 0 & 0 & 0 & 0\\
0 & 0 & 0 & 0 & 0 & -1.0\times10^{12} & -9.2\times10^{11} & -8.7\times10^{11} & -8.7\times10^{11} & -8.7\times10^{11} & 1.7\times10^{12} & -1.7\times10^{12} & 0 & 0 & 0\\
0 & 0 & 0 & 0 & 0 & 1.8\times10^{11} & 3.9\times10^{11} & 1.8\times10^{11} & 2.3\times10^{11} & 2.3\times10^{11} & -1.7\times10^{12} & 2.9\times10^{12} & -1.1\times10^{12} & 0 & 0\\
0 & 0 & 0 & 0 & 0 & -0.00015 & -5.2\times10^{11} & -1.8\times10^{11} & -5.2\times10^{10} & -0.00015 & 0 & -1.1\times10^{12} & 2.3\times10^{12} & -1.1\times10^{12} & 0\\
0 & 0 & 0 & 0 & 0 & -2.3\times10^{11} & -2.3\times10^{11} & -2.8\times10^{11} & -4.3\times10^{11} & -2.8\times10^{11} & 0 & 0 & -1.1\times10^{12} & 2.9\times10^{12} & -1.7\times10^{12}\\
0 & 0 & 0 & 0 & 0 & 8.7\times10^{11} & 8.7\times10^{11} & 8.7\times10^{11} & 8.3\times10^{11} & 7.0\times10^{11} & 0 & 0 & 0 & -1.7\times10^{12} & 1.7\times10^{13}
\end{bmatrix}$$

$$F=\begin{bmatrix}0\\0\\0\\0\\0\\6666.67\\8888.89\\8888.89\\8888.89\\6666.67\\0\\0\\0\\0\\0\end{bmatrix}\quad F_b=\begin{bmatrix}0\\0\\0\\0\\3.43\times10^{4}\\4\times10^{9}\\0\\0\\0\\0\\2.7\times10^{11}\\0\\0\\0\\0\end{bmatrix}$$

After the simulation of the deformable tower is put forward, the simulation result of the deformable tower is shown in Fig 10.

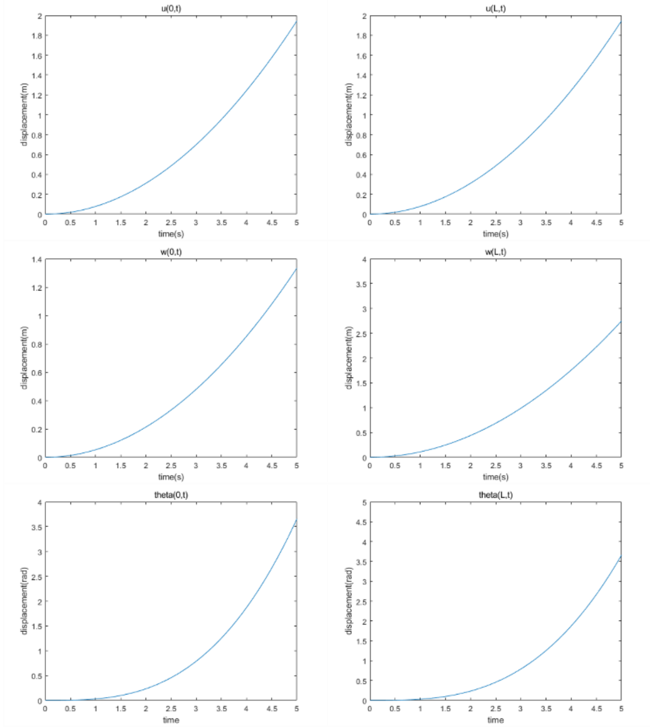

Fig. 10. Displacements of u, w and θ in both ends of the deformable tower

As it is shown in Fig 10, the bottom of the tower displaces less than the top of the tower in the direction of x and z. comparing with the displacement in z axis, the displacement in direction of x is less. The angular displacement of the bottom and top of the tower is quite familiar. The above observation derived from the simulation conforms with our intuition. While as time passing by, the displacement and angular displacement of the deformable tower increase which enhances the instability of the system. Therefore, researchers have carried out several control schemes and optimal designs to deal with the problem of stability control of the wind turbine generator in the complex environment [16-18].

REFERENCES

[1] He J, Jin X, Xie S Y, et al. Multi-body dynamics modeling and TMD optimization based on the improved AFSA for floating wind turbines[J]. Renewable Energy, 2019, 141: 305-321.

[2] Wayman E N, Sclavounos P D, Butterfield S, et al. Coupled dynamic modeling of floating wind turbine systems[C]. Offshore technology conference. Offshore Technology Conference, 2006.

[3] Musial W, Butterfield S, Boone A. Feasibility of floating platform systems for wind turbines[C]. 42nd AIAA aerospace sciences meeting and exhibit. 2004: 1007.

[4] Matha D. Model development and loads analysis of an offshore wind turbine on a tension leg platform with a comparison to other floating turbine concepts: April 2009[R]. National Renewable Energy Lab.(NREL), Golden, CO (United States), 2010.

[5] J. Name Stand. Abbrev. Jonkman J M. Dynamics modeling and loads analysis of an offshore floating wind turbine[R]. National Renewable Energy Lab.(NREL), Golden, CO (United States), 2007.

[6] Ishihara T, Namba H. Fem analysis and fatigue evaluation for the bolt joint between nacelle and tower top flange of a wind turbine[c]. Grand Renewable Energy proceedings Japan council for Renewable Energy (2018). Japan Council for Renewable Energy, 2018: 190.

[7] Martin H R. Development of a scale model wind turbine for testing of offshore floating wind turbine systems[J]. 2011.

[8] Larsen T J, Hanson T D. A method to avoid negative damped low frequent tower vibrations for a floating, pitch controlled wind turbine[C]. Journal of Physics: Conference Series. IOP Publishing, 2007, 75(1): 012073.

[9] Lackner M A. Controlling platform motions and reducing blade loads for floating wind turbines[J]. Wind Engineering, 2009, 33(6): 541-553.

[10] Butterfield S, Musial W, Jonkman J, et al. Engineering challenges for floating offshore wind turbines[R]. National Renewable Energy Lab.(NREL), Golden, CO (United States), 2007.

[11] Colherinhas G B, Shzu M A M, Avila S M, et al. Wind tower vibration controlled by a pendulum TMD using genetic optimization: beam modelling[J]. Procedia engineering, 2017, 199: 1623-1628.

[12] Adhikari S, Bhattacharya S. Vibrations of wind-turbines considering soil-structure interaction[J]. Wind and Structures, 2011, 14(2): 85.

[13] Piccardo G, Tubino F, Luongo A. Equivalent Timoshenko linear beam model for the static and dynamic analysis of tower buildings[J]. Applied Mathematical Modelling, 2019, 71: 77-95.

[14] Majkut L. Free and forced vibrations of Timoshenko beams described by single difference equation[J]. Journal of Theoretical and Applied Mechanics, 2009, 47(1): 193-210.

[15] Arany L, Bhattacharya S, Adhikari S, et al. An analytical model to predict the natural frequency of offshore wind turbines on three-spring flexible foundations using two different beam models[J]. Soil Dynamics and Earthquake Engineering, 2015, 74: 40-45.

[16] He W, Meng T, Liu J K, et al. Boundary control of a Timoshenko beam system with input dead-zone[J]. International Journal of Control, 2015, 88(6): 1257-1270.

[17] Yu J F, Wang B P. An optimization of frame structures with exact dynamic constraints based on Timoshenko beam theory[J]. Journal of sound and vibration, 2004, 269(3-5): 589-607.

[18] He W, Liu C. Vibration control of a Timoshenko beam system with input backlash[J]. IET Control Theory & Applications, 2015, 9(12): 1802-1809.